



High-capacity bi-directional full-duplex transmission based on fiber-eigenmode multiplexing over a FMF with 2×2 MIMO

JIANBO ZHANG,¹ XIONG WU,^{1,7} QIRUI FAN,² XINGWEN YI,^{3,8} ZHONGWEI TAN,⁴ JIANPING LI,⁵ ZHAOHUI LI,³ AND CHAO LU^{1,6}

¹Photonics Research Center, Department of Electronic and Information Engineering, The Hong Kong Polytechnic University, Hong Kong SAR, China

²Photonics Research Center, Department of Electrical Engineering, The Hong Kong Polytechnic University, Hong Kong SAR, China

³State Key Laboratory of Optoelectronic Materials and Technologies, School of Electronics and Information Technology, Sun Yat-sen University, Guangzhou 511400, China

⁴Key Laboratory of Photonic Information Technology, Ministry of Industry and Information Technology, School of Optics and Photonics, Beijing Institute of Technology, Beijing 100081, China

⁵School of Information Engineering, Guangdong University of Technology, Guangzhou 510632, China

⁶The Hong Kong Polytechnic University Shenzhen Research Institute, Shenzhen 518057, China

⁷xiong94.wu@connect.polyu.hk

⁸yixw5@mail.sysu.edu.cn

Abstract: We propose and experimentally demonstrate symmetrical (homo-modal) and asymmetrical (hetero-modal) full-duplex bi-directional architectures based on dual-vector eigenmodes multiplexing over a 3 km few mode fiber (FMF). Firstly, 4 vector modes (VMs) of 2 mode groups (MGs), $l = 0$ (HE_{11o} and HE_{11e} modes) and $l = +2$ (EH_{11o} and EH_{11e} modes), each carrying a 14 GBaud quadrature phase-shift keying (QPSK) signal, are utilized in the up and down links and a 224 Gb/s same-mode bi-directional transmission is successfully realized. The crosstalk between the VMs in $l = 0$ and $l = +2$ of this full-duplex system is less than -13.8 dB. To strengthen the immunity to performance degradation induced by connector reflection and back scattering, we propose an effective approach to mitigate impairments by using hetero-modes on two terminals of the bi-directional system. Then, 2 VMs of $l = 0$ and 2 VMs of $l = +2$ are respectively employed in the up and down streams. The channel isolation between the VMs in $l = 0$ and $l = +2$ of such full-duplex link is larger than 19 dB, which supports a 448 Gb/s bi-directional transmission with 28 GBaud 16-ary quadrature amplitude modulation (QAM) modulation over a 3 km FMF by using 2×2 MIMO. Moreover, mode-wavelength division multiplexing including 2 modes and 4 wavelengths in both up and down streams is implemented in the transmission system. A total capacity of the 1.792 Tb/s link with 28 GBaud 16-QAM signal over each channel is successfully realized over the 3 km FMF. The measured bit-error-ratios (BERs) of all channels are below the 7% hard decision forward error correction (FEC) threshold at 3.8×10^{-3} . The experimental results adequately indicate that such a scheme has a great potential in high-speed bi-directional point-to-point (P2P) optical interconnects.

© 2021 Optical Society of America under the terms of the [OSA Open Access Publishing Agreement](#)

1. Introduction

Over the past few decades, the advent of Internet of things (IoT), the evolution of bandwidth-hungry applications and the surge of global IP traffic have fueled the demands for high-speed high-capacity optical communication [1–3]. To keep pace with the information explosion, multiplexing technologies of wavelength and polarization have been proposed and applied to signal-mode fiber (SMF)-based commercial systems successfully. However, due to fundamental nonlinear Shannon limitation, the SMF-based architecture is approaching its scalability limit

and may no longer accommodate ever-growing data traffic in the future. More multiplexing dimensions should be exploited and utilized to enlarge the transmission capacity. Space-division multiplexing (SDM)/Mode-division multiplexing (MDM)-based technology in the multi-core fiber (MCF) or few mode fiber/multi-mode fiber (FMF/MMF) is regarded as a promising option to overcome current capacity bottleneck and remarkably upsurge the scalability of optical link [4–8]. In this proposal, the orthogonal fiber modes are exploited as parallel channels to carry independent signal and enlarge capacity density in an amount proportional to the number of co-transmitted fiber modes.

In the MDM link, since crosstalk induced by mode-coupling cannot be completely avoided among multiple mode channels, especially in the strongly-coupled mode channels, full multiple-input-multiple-output (MIMO) digital signal processing (DSP) is introduced to guarantee robust performance. However, the complexity of time domain MIMO DSP is increased squarely with the number of transmitted modes and is proportional to the number of taps in MIMO equalizer, which is determined by the maximum differential mode/mode-group delay. To reduce the computational complexity, weakly-coupled FMF/MMF-based MIMO-less scheme has been proposed [9,10]. MIMO-less is a tradeoff between full-MIMO with the best performance and MIMO-free with the least cost, in which MIMO block is only applied to equalize and demultiplex partial mode channels within same mode group (MG) or partial MGs with less MG isolation. Moreover, the transmission performance of different basis sets of fiber modes has also been investigated in detail, such as linearly polarized (LP) modes [11,12], orbital angular momentum (OAM) [6,13] and vector mode (VM) [14,15]. As the eigenmode of fiber, VM with spatially inhomogeneous state of polarization (SOP) has lately attracted much attention for its intrinsic characteristics. In fact, any other type of basis sets of fiber modes could be identified as the linear superposition of 2 orthogonal VMs. Besides, to further suppress mode crosstalk between/among MGs, specially-designed fibers that can stably guide OAM/VM have been widely investigated, such as ring-core fibers with circular symmetry [9,14]. Integrated optical vortex emitter, mode converter and mode multiplexer/de-multiplexer for eigenmode have also attracted lots of attention lately [14,16,17]. Thus, vector mode division multiplexing (VMDM)-based fiber transmission deserves more investigation and consideration.

Practical passive optical network (PON) is a typical bi-directional communication system case [18,19]. Wavelength-division-multiplexing (WDM)-PON is generally regarded as the most promising solution for the next generation access network [20,21]. On the other hand, it is worth noting that, for PONs, bi-directional link is a very important part, in which Rayleigh back scattering (RB) and Fresnel reflection (FR) that are the intrinsic processes of fibers will inevitably degrade the system performance [22,23]. In order to alleviate RB and FR effects, various bi-directional schemes have been proposed, such as wavelength offset detuning [24,25], frequency dithering [26,27], cross-remodulation schemes [28,29] and time-division-duplexing (TDD) [30,31]. However, the performance upgradation based on these scenarios requires extra bandwidth or extra laser sources or time-sharing basis, which will definitely result in low spectral efficiency (SE) and resource-wasting. Undoubtedly, future fiber-optic network is expected to achieve higher performance, higher capacity, and higher bandwidth utilization. Thus, MDM-based bi-directional transmission merits more focus. Although there have been several works that demonstrate the feasibility of LP/OAM-based MDM bi-directional links [32–34], the system limitation and optimization are not widely investigated and discussed.

In this paper, by employing the direct fiber eigenmodes, vector modes, we propose, demonstrate, and evaluate two architectures of VMDM-based full-duplex full-polarization bi-directional transmission over 3 km FMF. Firstly in Section 2, we evaluate and analyze the degradation of back crosstalk from FMF. Both uplink and downlink transmit 4 VMs belonging to 2 MGs: $l = 0$ and $l = +2$. The full-duplex crosstalk of this system is less than -13.8 dB. Accordingly, each mode channel carries 14 GBaud quadrature phase-shift keying (QPSK) signal and a 224 Gb/s

bi-directional transmission over 3 km FMF is demonstrated, using a 2×2 complex MIMO only for each MG with only 5 taps of 2×2 MIMO finite-impulse-response (FIR) filter. Secondly in Section 3, in order to enhance the tolerance against back crosstalk, we propose a simple and effective approach by utilizing the hetero-modes on two ends of bi-directional transmission. 2 VMs of $l = 0$ and 2 VMs of $l = +2$ are respectively loaded in the uplink and downlink with isolation between counter direction larger than 19 dB. Then, a 448 Gb/s full-duplex bi-directional VMDM link with 28 GBaud 16-ary quadrature amplitude modulation (16-QAM) is demonstrated over 3 km FMF, using a 9-tap 2×2 MIMO equalizer. Moreover, Section 4 presents a 1.792 Tb/s four-wavelength WDM-VMDM full-duplex bi-directional link, based on the same hetero-modal scheme. All experimental results meet the 7% hard decision forward error correction (FEC) bit-error-ratio (BER) of 3.8×10^{-3} , emphasizing that the proposed hetero-modal scheme could be a competitive candidate for future high-SE high-capacity bi-directional transmission link.

2. Full-duplex homo-VMs based MDM bi-directional link

Figure 1 illustrates the homo-mode based full-duplex bi-directional transmission over 3 km FMF, in which identical 4 VMs are transmitted on both uplink and downlink. At each transmitter (Tx1/Tx2), the continuous wavelength (CW) light-wave from the external cavity lasers (ECL, 1550.12 nm, ~100 kHz linewidth) is split into 2 branches by a 1:1 optical coupler (OC). One branch is used as the local oscillator (LO) for the opposite transmission signal by coherent detection. Another branch is fed into the I/Q modulator driven by the 14 GBaud QPSK signal, which is shaped spectrally with a 0.5 roll-off factor (RF) raised-cosine (RC) filter and generated by an arbitrary waveform generator (AWG, Keysight M8196A), operating at 84 GSa/s sampling rate. After amplified by an erbium-doped fiber amplifier (EDFA), polarization division multiplexing (PDM) is emulated by polarization beam splitters (PBS) and polarization beam combiner (PBC). The polarization controller (PC) after EDFA is utilized to balance the power of horizontal and vertical light beams of PDM. Then, the mutually orthogonal signals are split into 2 parts by a 1:1 OC. One is employed to generate VMs of $l = +2$ (EH_{11o} and EH_{11e} modes) by vortex wave plate (VWP) and another is directly employed as VMs of $l = 0$ (HE_{11o} and HE_{11e} modes). Next, 4 VMs are multiplexed together by a beam splitter (BS) and coupled into the 3 km FMF through a collimator (COL). Here, the fiber coupling loss is about 3 dB including the COL. In our experiment, the step-index FMF with a core diameter of 19 μm and a cladding diameter of 125 μm is utilized. The refractive indices of the core and cladding of the FMF are 1.449 and 1.444, respectively and the transmission loss of this FMF is about 0.25 dB/km. The used 4 VMs ($l = 0$ and $l = +2$) and the calculated effective refractive index (n_{eff}) of used VMs in that the effective refractive index difference Δn_{eff} between VM of $l = 0$ and $l = +2$ is around 3×10^{-3} . Such relatively large Δn_{eff} indicates that the couplings between VMs of $l = 0$ and $l = +2$ are low when they are multiplexed and transmitted in this FMF. In the FMF link, a FMF-based PC (PC-FMF) is utilized to adjust the polarization and intensity distribution of the output beams for the optimal pattern. In Fig. 1, insets (I) to (IV) and (V) to (VIII) respectively show the captured intensity profiles of uplink and downlink for VM channels after 3 km FMF transmission. After full-duplex fiber transmission, the light beams are separated into 2 parts by another BS. One branch is directly fed into the SMF to filter higher-order VMs and only VMs of $l = 0$ with mutually orthogonal SOPs can be detected. In another branch, VMs of $l = +2$ are converted back to the orthogonal fundamental modes after passing through the VWP. Meanwhile, VMs of $l = 0$ are transferred to higher-order VMs that cannot be coupled into SMF. In this way, VMs of $l = 0$ and $l = +2$ are separated and are sent to the corresponding receiver.

At each receiver (Rx1/Rx2), dual-polarized signals and LO are sent to dual-polarization (DP) 90° hybrid for coherent detection after a circulator (CIR). The laser of Tx2/Tx1 can be served as LO in Rx1/Rx2 for the sake of same wavelength used in both ends. Then, 4 electrically-received signals after 4 balanced photo-detectors (PDs) go through the offline DSP which accordingly

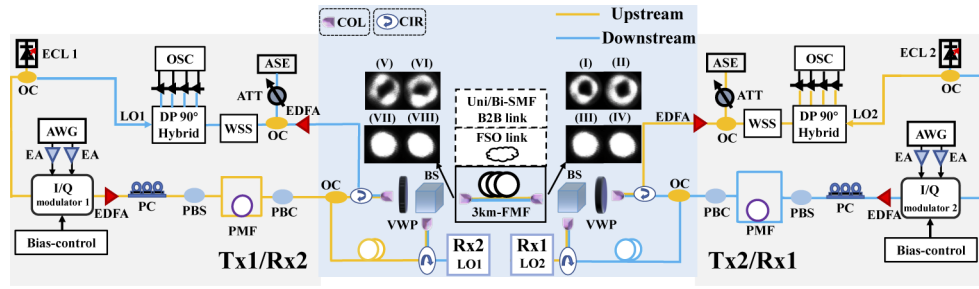


Fig. 1. The experimental setup of full-duplex homo-VMs based MDM bi-directional transmission. AWG: arbitrary waveform generator; EA: electrical amplifier; ECL: external cavity laser; OC: optical coupler; EDFA: erbium-doped fiber amplifier; PC: polarization controller; PBS: polarization beam splitter; PBC: polarization beam combiner; PMF: polarization maintaining fiber; CIR: circulator; COL: collimator; VWP: vortex wave plate; BS: beam splitter; FMF: few-mode fiber; ATT: attenuator; WSS: wavelength selective switch; ASE: amplifier spontaneous-emission noise; OSC: oscilloscope; LO: local oscillator; B2B: back-to-back; FSO: free space optical.

includes resampling, fractionally-spaced 2×2 constant modulus algorithm (CMA) for adaptively demultiplexing and equalizing of dual-polarized signals [35], frequency offset estimation using the periodogram of the 4th power of equalized signals [36], carrier phase recovery, BER calculation and signal-to-noise ratio (SNR) calculation. Here, the number of taps in CMA is set to 5, which is enough to compensate the differential group delay (DGD) and other inter-symbol interference (ISI) within same order VMs after 3 km FMF transmission.

Figure 2 shows the measured crosstalk of 2 used VM MGs in this full-duplex system based on the power measurement, including uni-directional crosstalk and bi-directional crosstalk. For uni-directional transmission, the isolation between the 2 VM MGs of uni-directional is larger than 18.5 dB. Inter-modal crosstalk could be introduced when VMs are coupling into FMF from free space, because it is hard to realize perfect vertical incidence. Besides, channel crosstalk may be caused by the fiber perturbation and imperfection, which could further lead to mode degradation. For bi-directional link, except for uni-directional crosstalk mentioned before, counterpropagating signals of same wavelength and homo-mode unavoidably suffer severe deterioration. In our experiment, crosstalk caused by RB is very slightly due to short-reach FMF. FR, especially connector (FC/PC, made of ourselves) reflection, is mainly accountable for crosstalk between same modes in the counter direction. As it can be seen, the measured bi-directional crosstalk from the counter direction is less than -13.8 dB, which is the major impairment for the whole system.

To further evaluate the transmission performance of this VMDM-based bi-directional system, we respectively measure the BER property versus the optical signal-to-noise power ratio (OSNR) under SMF back-to-back (B2B), bi-directional SMF B2B, bi-directional free space optical (FSO) and bi-directional FMF link cases. Here, the B2B case is the DP signals are directly sent to the receiver. The measured BER performance of DP signals for VMs of $l = 0$ and $l = +2$ under uplink (BiU0/BiU2) and downlink (BiD0/BiD2) transmission are plotted with up-pointing triangles and down-pointing triangles, respectively, in Fig. 3, using 14 GBaud QPSK for each mode with the aggregate capacity of 224 Gb/s ($14 \times 2 \times 4 \times 2$ (directions) = 224 Gb/s). The BER performance of VMs of $l = 0$ is always better than that of VMs of $l = +2$ under two cases. Compared with uni/bi-directional B2B and bi-directional FSO links (hollow/filled circles and hollow triangles in Fig. 3), the power penalties for uplink and downlink are respectively about 6/6/5 dB and 5/5/4 dB of VMs of $l = 0$ under the 7% hard decision FEC threshold of 3.8×10^{-3} BER. As for VMs of $l = +2$, the power penalties are about 8/8/6.5 dB and 8.5/8.5/7 dB respectively for uplink and

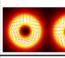
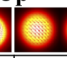
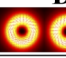
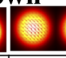

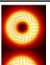
Mode crosstalk (dB)	Up		Down		
					
	0	-19.7	-15.2	-19.3	 Up
	-20	0	-19.8	-13.8	
	-14.9	-21.1	0	-19.6	 Down
	-19	-14.3	-18.5	0	

Fig. 2. The normalized mode crosstalk matrix for such full-duplex VMDM bi-directional system.

downlink at BER of 3.8×10^{-3} . Such penalties are mainly induced by back crosstalk, which is also the key limitation for system capacity.

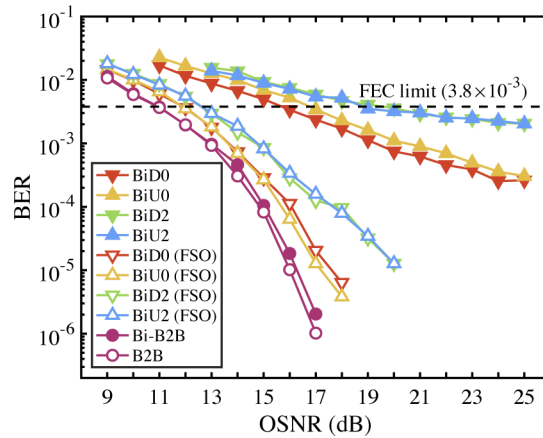


Fig. 3. Measured BER versus OSNR of 14 GBaud QPSK for 4 homo-VMs based MDM bi-directional transmission.

In order to suppress the back crosstalk of bi-directional system, wavelength offset detuning [24,25] is a simple and general method, in which wavelengths transmission in opposite direction are sufficiently spaced to alleviate RB and FR effect. Here, to verify the impact of wavelengths offset for VMDM bi-directional link, we respectively adjust the wavelength of VM channels in uplink and downlink. It is noted that only one identical VM MG in each end is transmitted each time to exclude impacts from other interferences. Figure 4 plots the calculated SNR as a function of wavelength offset when 2 VMs of $l = 0$ or $l = +2$ are transmitted bi-directionally. We can find that SNR is significantly improved when the wavelength offset is larger than signal's bandwidth $14 \times (1 + 0.5) = 21$ GHz (~ 0.168 nm).

For bi-directional transmission, with implementation of same wavelengths and modes, counterpropagating signals suffer from back crosstalk. In the wavelength detuning scheme, the performance upgradation is based on extra bandwidth, which will result in low SE. Admittedly,

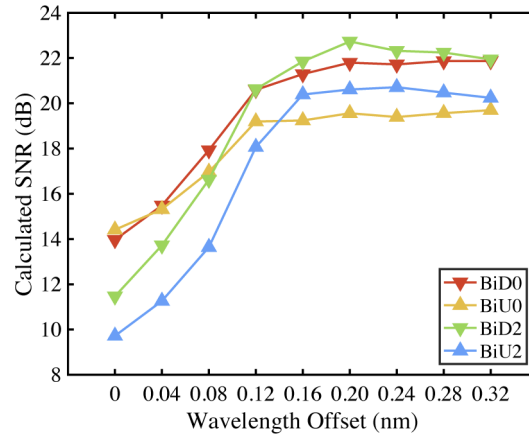


Fig. 4. Calculated SNR performance versus wavelength offset when VMs of $l = 0$ or $l = +2$ are transmitted bi-directionally.

hetero-mode full-duplex architecture is also a kind of wasting the space dimension. Nevertheless, the hetero-mode architecture shows a better choice. First, it enables wavelength dimension to be fully utilized. Compared with space dimension, wavelength dimension is now more scalable and mature. Second, for coherent detection with higher SE, same wavelength in the uplink and downlink can be utilized as LO for counter direction at the Rx. On the contrary, this wavelength detuning scheme requires extra laser source as for LO, leading to extra cost or complexity. In addition, this scheme is at the price of bandwidth exhaust, which will be no longer satisfy future bandwidth-hungry applications in full-duplex WDM-PON. Thus, hetero-mode same-wavelength scheme is a suitable tradeoff.

3. Full-duplex hetero-VMs based MDM bi-directional link

To further enhance system immunity to opposite-directional signal degradation, a simple and effective scheme by employing hetero-VMs on two ends of bi-directional transmission is demonstrated. The experimental setup of full-duplex hetero-VMs based MDM bi-directional link is also based on Fig. 2 and the simplified schematic diagram is shown in Fig. 5. Here, 2 VMs of $l = +2$ and 2 VMs of $l = 0$ are respectively employed in the uplink and downlink. As it can be seen in Fig. 2, the bi-directional crosstalk for hetero-VMs MGs is less than -19 dB. Accordingly, 28 GBaud 16-QAM signals with 0.1 RF RC filter are modulated on the used VMs on two terminals. At the receiver, different from DSP for homo bi-directional QPSK signal in Section 2, 2×2 CMA is only used for pre-equalization in-tandem with a 2×2 radius directed equalizer (RDE) [37] performed for further adaptive equalization of 16-QAM signal. The number of taps used for CMA and RDE are both set to 9, which, for fair comparison, covers the same ISI duration as 5 taps in 14 GBaud QPSK in Section 2.

Then, we evaluate the BER performance over single wavelength (1550.12 nm) bi/uni-directional transmission with uni-directional SMF B2B transmission carrying DP signals for comparison. The BER versus OSNR of used VM MGs for bi/uni-direction are plotted with triangles/circles in Fig. 6. There is about 1.1 dB/1.3 dB power penalty can be seen between the uni-directional uplink (UniU2) /downlink (UniD0) and B2B (hollow circles in Fig. 6). Under bi-directional transmission, there are just around 3.8 dB and 4 dB power penalties for uplink (BiU2) and downlink (BiD0) referring to uni-directional SMF B2B, respectively. The constellation diagrams of the demodulated 16-QAM signals for full-duplex uplink and downlink at the OSNR of 32 dB

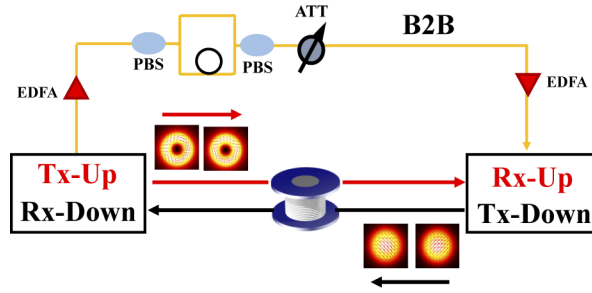


Fig. 5. Schematic diagram of full-duplex hetero-VMs based MDM bi-directional link.

are shown in Fig. 6(I) and (II), respectively. The data capacity of this demonstration is 448 Gb/s ($28 \times 4 \times 2 \times 2$ (directions) = 448 Gb/s).

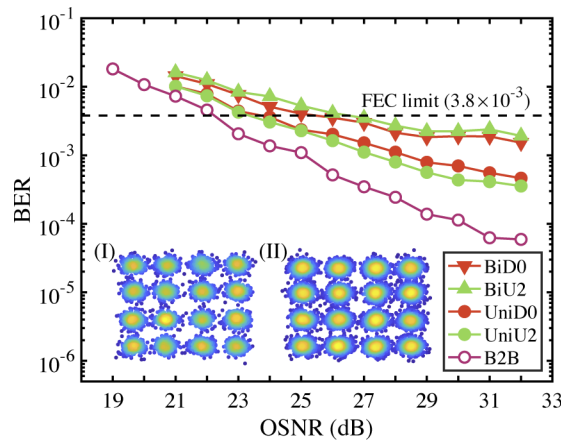


Fig. 6. Measured BER versus OSNR of 28 GBaud 16-QAM for hetero-VMs based MDM bi-directional transmission.

Compared with homo-modal scheme, the hetero-modal scheme doubles the overall data capacity of bi-directional transmission enabling higher baud-rate (28 GBaud) and higher modulation format (16-QAM), which indicates this scheme can be further applied to longer distance transmission.

4. Full-duplex hetero-VMs based MDM-WDM bi-directional link

Hetero-modal scheme is also compatible with the existed WDM systems and enables the wavelength resource to be fully explored. To further demonstrate the reliability and feasibility of the proposed hetero-VMs based bi-directional scheme, we therefore conduct the hetero-VMs WDM bi-directional system. Figure 7 shows the schematic of full-duplex hetero-VMs based MDM-WDM transmission. In this configuration, at each transmitter 4 wavelengths (ranging from 1549.72 nm to 1550.92 nm, λ_1 to λ_4) from 4 ECLs (~ 100 kHz linewidth) in a 0.4 nm/50 GHz grid are combined by a wavelength division multiplexer. Then, 4 optical carriers are modulated by 28 GBaud 16-QAM signal using a RC filter with a RF of 0.1. PDM for generated signal is enabled by a PDM emulator (PDME). Subsequently, by employing VWP, uplink beams are converted to the VMs of $l = +2$ and then coupled into the FMF after a BS. Downlink beams are directly employed as VMs of $l = 0$ and are coupled into FMF.

After 3 km full-duplex FMF transmission, followed by the BS, uplink beams are converted back to the orthogonal polarizations by another VWP for detection. Meanwhile, downlink beams

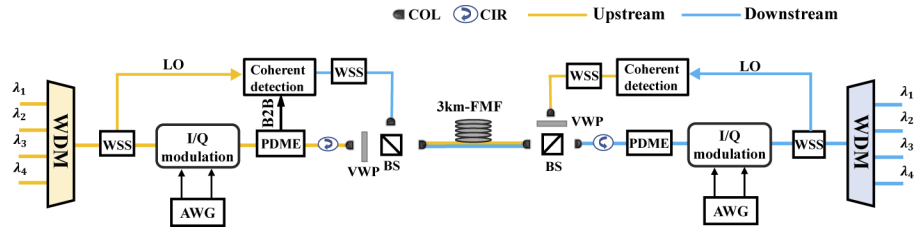


Fig. 7. The experimental setup of full-duplex hetero-VMs based MDM-WDM bi-directional transmission.

can be directly sent to the receiver for coherent detection. At each receiver, LO and signals from the opposite direction are filtered accordingly by wavelength selective switch (WSS) and then are sent to the receiver for coherent detection and DSP.

The BER performance for bi/uni-directional transmission is shown in Fig. 8. The inset (I) of Fig. 8 depicts the corresponding optical spectrum of the 4 WDM channels of 28 GBaud 16-QAM. It can be seen that the BER values of VMs of $l = +2$ (uplink) and VMs of $l = 0$ (downlink) at 4 different wavelengths are all below the FEC threshold of 3.8×10^{-3} with the total capacity of 1.792 Tb/s ($28 \times 4 \times 2 \times 4 \times 2$ (directions) = 1.792 Tb/s). This realization further indicates that this scheme exhibits robust performance and presents powerful extensibility. What's more, with the development of specially-designed FMF/MMF for VM and OAM and the corresponding mode multiplexer/de-multiplexer, bi-directional MDM link with more mode channels could be realized and it is a powerful candidate for future full-duplex PON with the requirement of high-capacity.

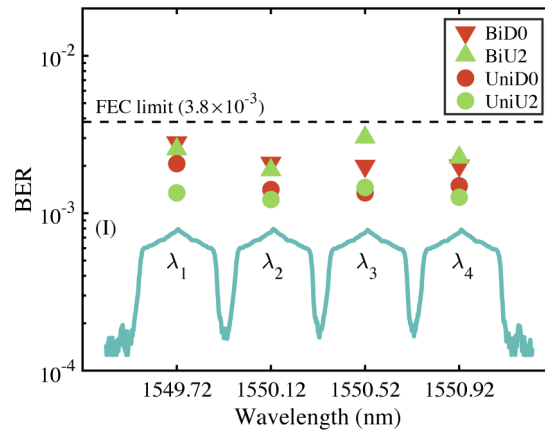


Fig. 8. Measured BER performance of all 16 channels for MDM-WDM bi-directional transmission.

5. Conclusions

In this paper, we experimentally demonstrate fiber eigenmode-based MDM full-duplex bi-directional transmission over 3 km FMF. Two bi-directional architectures of homo-VMs and hetero-VMs transmitted in two directions are implemented based on coherent detection and 2×2 MIMO DSP. First, both uplink and downlink transmit 4 identical vector modes. Due to the same-mode crosstalk caused by RB and FR of this full-duplex system, each mode channel is only able to carry 14 GBaud QPSK signal and a 224 Gb/s bi-directional link over 3 km FMF is demonstrated. Then, we propose the second scheme of employing different VMs on two ends to

minimize the impact from back crosstalk on the same mode. 2 dual-polarization VMs of $l = 0$ and 2 dual-polarization VMs of $l = +2$ are respectively loaded in the up and down streams. The isolation between opposite direction is larger than 19 dB and a 448 Gb/s bi-directional VMDM transmission is demonstrated over 3 km FMF. Obviously, compared with the first demonstration, this scheme doubles the transmission capacity under the same hardware conditions. Furthermore, by combining WDM technology, a 1.792 Tb/s WDM-VMDM full-duplex bi-directional system with 4 wavelengths on the two ends is successfully achieved. The experimental results present that the proposed method could find enormous potential in future larger-scale optical interconnects.

Funding. National Key Research and Development Program of China (2018YFB1801701); National Natural Science Foundation of China (62022029, U1701661); Program for Guangdong Introducing Innovative and Entrepreneurial Teams (2019ZT08X340); Research and Development Plan in Key Areas of Guangdong Province (2018B010114002); State Key Laboratory of Advanced Optical Communication Systems and Networks, China (2019GZKF1).

Disclosures. The authors declare no conflicts of interest.

Data availability. Data underlying the results presented in this paper are not publicly available at this time but may be obtained from the authors upon reasonable request.

References

1. R.-J. Essiambre, G. Kramer, P. J. Winzer, G. J. Foschini, and B. Goebel, "Capacity Limits of Optical Fiber Networks," *J. Lightwave Technol.* **28**(4), 662–701 (2010).
2. P. J. Winzer, "Scaling Optical Fiber Networks: Challenges and Solutions," *Opt. Photonics News* **26**(3), 28–35 (2015).
3. G. Li, N. Bai, N. Zhao, and C. Xia, "Space-division multiplexing: the next frontier in optical communication," *Adv. Opt. Photonics* **6**(4), 413–487 (2014).
4. J. Li, J. Zhang, F. Li, X. Huang, S. Gao, and Z. Li, "DD-OFDM transmission over few-mode fiber based on direct vector mode multiplexing," *Opt. Express* **26**(14), 18749–18757 (2018).
5. J. Zhang, J. Liu, L. Shen, L. Zhang, J. Luo, J. Liu, and S. Yu, "Mode-division multiplexed transmission of wavelength-division multiplexing signals over a 100-km single-span orbital angular momentum fiber," *Photonics Res.* **8**(7), 1236–1242 (2020).
6. A. Wang, L. Zhu, L. Wang, J. Ai, S. Chen, and J. Wang, "Directly using 8.8-km conventional multi-mode fiber for 6-mode orbital angular momentum multiplexing transmission," *Opt. Express* **26**(8), 10038–10047 (2018).
7. G. Rademacher, B. J. Puttnam, R. S. Luís, J. Sakaguchi, W. Klaus, T. A. Eriksson, Y. Awaji, T. Hayashi, T. Nagashima, T. Nakanishi, T. Taru, T. Takahata, T. Kobayashi, H. Furukawa, and N. Wada, "10.66 Peta-Bit/s Transmission over a 38-Core-Three-Mode Fiber," in *Optical Fiber Communication Conference (OFC) 2020*, (Optical Society of America, 2020), p. Th3H.1.
8. A. V. Turukhin, O. V. Sinkin, H. G. Batshon, Y. Sun, M. Mazurczyk, C. R. Davidson, J.-X. Cai, M. A. Bolshtyansky, D. G. Foursa, and A. N. Pilipetskii, "High Capacity Ultralong-Haul Power Efficient Transmission Using 12-Core Fiber," *J. Lightwave Technol.* **35**(4), 1028–1032 (2017).
9. G. Zhu, Z. Hu, X. Wu, C. Du, W. Luo, Y. Chen, X. Cai, J. Liu, J. Zhu, and S. Yu, "Scalable mode division multiplexed transmission over a 10-km ring-core fiber using high-order orbital angular momentum modes," *Opt. Express* **26**(2), 594–604 (2018).
10. J. Liang, Q. Mo, S. Fu, M. Tang, P. Shum, and D. Liu, "Design and fabrication of elliptical-core few-mode fiber for MIMO-less data transmission," *Opt. Lett.* **41**(13), 3058–3061 (2016).
11. H. Wen, C. Xia, A. M. Velázquez-Benítez, N. Chand, J. E. Antonio-Lopez, B. Huang, H. Liu, H. Zheng, P. Sillard, X. Liu, F. Effenberger, R. Amezcua-Correa, and G. Li, "First Demonstration of Six-Mode PON Achieving a Record Gain of 4 dB in Upstream Transmission Loss Budget," *J. Lightwave Technol.* **34**(8), 1990–1996 (2016).
12. Z. Wu, J. Li, D. Ge, F. Ren, P. Zhu, Q. Mo, Z. Li, Z. Chen, and Y. He, "Demonstration of all-optical MDM/WDM switching for short-reach networks," *Opt. Express* **24**(19), 21609–21618 (2016).
13. H. Huang, G. Milione, M. P. J. Lavery, G. Xie, Y. Ren, Y. Cao, N. Ahmed, T. A. Nguyen, D. A. Nolan, M.-J. Li, M. Tur, R. R. Alfano, and A. E. Willner, "Mode division multiplexing using an orbital angular momentum mode sorter and MIMO-DSP over a graded-index few-mode optical fibre," *Sci. Rep.* **5**(1), 14931 (2015).
14. J. Liu, S.-M. Li, L. Zhu, A.-D. Wang, S. Chen, C. Klitis, C. Du, Q. Mo, M. Sorel, S.-Y. Yu, X.-L. Cai, and J. Wang, "Direct fiber vector eigenmode multiplexing transmission seeded by integrated optical vortex emitters," *Light: Sci. Appl.* **7**(3), 17148 (2018).
15. J. Zhang, X. Wu, L. Lu, J. Li, J. Tu, Z. Li, and C. Lu, "1.12 Tbit/s fiber vector eigenmode multiplexing transmission over 5-km FMF with Kramers-Kronig receiver, in Optical Fiber Communication Conference (OFC) 2020," (Optical Society of America, 2020), p. W1D.5.
16. Y. Chen, L. A. Rusch, and W. Shi, "Integrated Circularly Polarized OAM Generator and Multiplexer for Fiber Transmission," *IEEE J. Quantum Electron.* **54**(2), 1–9 (2018).
17. Y. Wen, I. Chremmos, Y. Chen, G. Zhu, J. Zhang, J. Zhu, Y. Zhang, J. Liu, and S. Yu, "Compact and high-performance vortex mode sorter for multi-dimensional multiplexed fiber communication systems," *Optica* **7**(3), 254–262 (2020).

18. A. Rashidinejad, A. Nguyen, M. Olson, S. Hand, and D. Welch, "Real-Time Demonstration of 2.4Tbps (200Gbps/) Bidirectional Coherent DWDM-PON Enabled by Coherent Nyquist Subcarriers," in *Optical Fiber Communication Conference (OFC) 2020*, (Optical Society of America, 2020), p. W2A.30.
19. C.-H. Lee, W. V. Sorin, and B. Y. Kim, "Fiber to the Home Using a PON Infrastructure," *J. Lightwave Technol.* **24**(12), 4568–4583 (2006).
20. F.-T. An, K. S. Kim, D. Gutierrez, S. Yam, E. Hu, K. Shrikhande, and L. Kazovsky, "SUCCESS: a next-generation hybrid WDM/TDM optical access network architecture," *J. Lightwave Technol.* **22**(11), 2557–2569 (2004).
21. H. Rohde, E. Gottwald, A. Teixeira, J. D. Reis, A. Shahpari, K. Pulverer, and J. S. Wey, "Coherent ultra dense wdm technology for next generation optical metro and access networks," *J. Lightwave Technol.* **32**(10), 2041–2052 (2014).
22. M. Nakazawa, "Rayleigh backscattering theory for single-mode optical fibers," *J. Opt. Soc. Am.* **73**(9), 1175–1180 (1983).
23. Z. Wang, H. Wu, X. Hu, N. Zhao, Q. Mo, and G. Li, "Rayleigh scattering in few-mode optical fibers," *Sci. Rep.* **6**(1), 35844 (2016).
24. T. Gui, X. Wang, M. Tang, Y. Yu, Y. Lu, and L. Li, "Real-Time Demonstration of 600 Gb/s DP-64QAM SelfHomodyne Coherent Bi-Direction Transmission with Un-Cooled DFB Laser," in *Optical Fiber Communication Conference Postdeadline Papers 2020*, (Optical Society of America, 2020), p. Th4C.3.
25. T. Zami, B. Lavigne, O. B. Pardo, S. Weisser, J. David, M. L. Monnier, and J.-P. Faure, "31.2-Tb/s real time bidirectional transmission of 78x400 Gb/s interleaved channels over C band of one 90-km SMF span," in *Optical Fiber Communication Conference*, (Optical Society of America, 2018), p. W1B.5.
26. J. A. Lazaro, C. Arellano, V. Polo, and J. Prat, "Rayleigh Scattering Reduction by Means of Optical Frequency Dithering in Passive Optical Networks With Remotely Seeded ONUs," *IEEE Photonics Technol. Lett.* **19**(1), 64–66 (2007).
27. D. Kim, B. G. Kim, T. Bo, and H. Kim, "80-km Reach 28-Gb/s/λ RSOA-based Coherent WDM PON Using Dither-Frequency-Tuning SBS Suppression Technique," in *Optical Fiber Communication Conference (OFC) 2019*, (Optical Society of America, 2019), p. Th3F.6.
28. H.-H. Lin, C.-Y. Lee, S.-C. Lin, S.-L. Lee, and G. Keiser, "WDM-PON Systems Using Cross-Remodulation to Double Network Capacity with Reduced Rayleigh Scattering Effects," in *Optical Fiber Communication Conference/National Fiber Optic Engineers Conference*, (Optical Society of America, 2008), p. OTuH6.
29. C. H. Yeh, C. W. Chow, and H. Y. Chen, "Simple Colorless WDM-PON With Rayleigh Backscattering Noise Circumvention Employing m -QAM OFDM Downstream and Remodulated OOK Upstream Signals," *J. Lightwave Technol.* **30**(13), 2151–2155 (2012).
30. L. Hu, G. Wu, H. Zhang, and J. Chen, "A 300-kilometer optical fiber time transfer using bidirectional TDM dissemination," in *Proceedings of the 46th Annual Precise Time and Time Interval Systems and Applications Meeting*, (2014), pp. 41–44.
31. V. Houtsma and D. van Veen, "Bi-Directional 25G/50G TDM-PON With Extended Power Budget Using 25G APD and Coherent Detection," *J. Lightwave Technol.* **36**(1), 1 (2017).
32. J. Sakaguchi, W. Klaus, Y. Awaji, N. Wada, T. Hayashi, T. Nagashima, T. Nakanishi, T. Taru, T. Takahata, and T. Kobayashi, "228-Spatial-Channel Bi-Directional Data Communication System Enabled by 39-Core 3-Mode Fiber," *J. Lightwave Technol.* **37**(8), 1756–1763 (2019).
33. S. Chen, J. Liu, Y. Zhao, L. Zhu, A. Wang, S. Li, J. Du, C. Du, Q. Mo, and J. Wang, "Full-duplex bidirectional data transmission link using twisted lights multiplexing over 1.1-km orbital angular momentum fiber," *Sci. Rep.* **6**(1), 38181 (2016).
34. T. Hu, J. Li, K. Zhang, F. Ren, Q. Mo, Y. Ke, C. Du, Z. Liu, Y. He, Z. Li, and Z. Chen, "Experimental Demonstration of Bidirectional MDM-WDM-TDM-PON Over Low Modal-crosstalk FMF," in *Optical Fiber Communication Conference*, (Optical Society of America, 2016), p. M3C.2.
35. M. Selmi, Y. Jaouen, and P. Ciblat, "Accurate digital frequency offset estimator for coherent PolMux QAM transmission systems," in *2009 35th European Conference on Optical Communication*, (2009), pp. 1–2.
36. D. Godard, "Self-Recovering Equalization and Carrier Tracking in Two-Dimensional Data Communication Systems," *IEEE Trans. Commun.* **28**(11), 1867–1875 (1980).
37. M. Ready and R. Gooch, "Blind equalization based on radius directed adaptation," in *International Conference on Acoustics, Speech, and Signal Processing*, (1990), pp. 1699–1702 vol.3.